ISSN 2078-5615. Вісник Львівського університету. Серія хімічна. 2026. Випуск 67. С. 3–21
Visnyk of the Lviv University. Series Chemistry. 2026. Issue 67. P. 3–21

Неорганічна хімія

УДК 669.018+548.736.4

THE SYSTEM Tb–Co–C AT 800 °C: PHASE EQUILIBRIA AND CRYSTAL STRUCTURE OF COMPOUNDS

V. Levytskyi[1], V. Babizhetskyy[2], B. Kotur[2]

[1]*Institut für Experimentelle Physik, TU Bergakademie Freiberg, Leipziger Str., 23, 09599 Freiberg, Germany;*

[2]*Department of Inorganic Chemistry, Ivan Franko National University of Lviv, Kyryla i Mefodiya Str., 6, UA–79005 Lviv, Ukraine*
[*]*e-mail: bohdan.kotur@lnu.edu.ua*

The isothermal section of the Tb–Co–C phase diagram at 800 °C has been studied in the range Co–C–Tb_2C–$TbCo_2$ using powder X-ray phase and structure analyses, energy-dispersive X-ray spectroscopy, and differential thermal analysis (for $TbCo_5$ composition). Four ternary compounds $TbCoC_2$, TbCoC, $Tb_4Co_2C_3$, $Tb_8Co_4C_9$ and nine binary compounds Tb_2Co_{17}, Tb_2Co_7, $TbCo_3$, $TbCo_2$, TbC_2, Tb_2C_3, Tb_3C_4, Tb_4C_5, Tb_2C have been found to exist at 800 °C. Binary compound $TbCo_5$ is thermodynamically stable in the limited temperature range at temperatures above 800 °C and melts congruently at 1331 °C. The crystal structure of ternary compounds are the following: $TbCoC_2$ (structure type (ST) $CeNiC_2$), TbCoC (ST YCoC, space group (SG) $P4_2/mmc$; the crystal structure was refined using powder XRD data), $Tb_4Co_2C_3$ (ST $Tb_4Co_2C_3$), $Tb_8Co_4C_9$ (original ST, SG $P2/m$; a = 13.5621(2) Å, b = 3.64432(9) Å, c = 7.0691(1) Å, β = 105.241(3), according to X-ray powder diffraction data).

Keywords: phase equilibria, ternary terbium cobalt carbides, crystal structure.

DOI: https://doi.org/10.30970/vch.6701.003

1. Introduction

Studies of ternary *R*–*T*–C (*R* = rare earth element, *T* = transition element) systems and binary and ternary carbides have become of high interest due to the variety of fascinating chemical and physical properties they exhibit [1–3]. Above 400 ternary *R*–*T*–C phases have been synthesized, and the crystal structure of the majority of them has been studied. The latest comprehensive overview of known *R*–*T*–C systems, including literature data and the authors own experimental results, was compiled in Ref. [3]. A systematic investigation of multicomponent systems is a practical approach for discovering new compounds. We continue our systematic studies on the *R*–*T*–C (*T* = 3*d*-element) systems, focusing on their potential for developing new functional and energy-efficient materials, as described in [4].

Among the ternary *R*−Co−C systems, the isothermal sections in the entire concentration range have been studied for the following *R*-systems: Sc at 600 °C [5], Y, La, and Ce at 400 °C [6], Dy at 800 °C and partially at 700 °C in the range 38−75 at. % Dy and 0−10 at. % C [7], for Gd at 600 °C [8] and for Er at 800 °C in the concentration range Co−C−Er_2C− $ErCo_2$ [9]. For the systems *R* = Y, La→Nd, Sm, and Gd→Lu, isothermal sections at 827 °C in the range Co−C−RC_2−RCo_5 were studied [10]. For Sm, isothermal sections were examined at 900 °C in the range 0−50 at. % Sm [11]. In the indicated systems, one to four ternary compounds occur. These data are shown in Table 1. Some ternaries were synthesised under different conditions compared to the studied sections of the phase diagrams. This suggests that some ternary compounds are likely to exist in limited temperature ranges. More detailed information on the studied isothermal sections of phase diagrams and crystallographic characteristics of the *R*−Co−C (*R* = rare earth) ternary compounds is given in [3].

Table 1

Characteristics of the *R*–Co–C (*R* = rare earth) ternary compounds

R Compounds	Sc	Y	La	Ce	Pr	Nd	Sm	Eu	Gd	Tb	Dy	Ho	Er	Tm	Yb	Lu
*R*CoC *ST YCoC		+							+	+	+	+	+	+	+	+
$RCoC_2$ ST $CeCoC_2$ ST $CeNiC_2$ ST $ScCoC_2$	+	+	+	+	+	+	+ LTM + HTM		+	+	+	+	+	+	+	+
R_2CoC_2/$R_4Co_2C_3$ ST $Tb_4Co_2C_3$		+							+	+	+	+				
$ScCo_3C$ ST $CaTiO_3$	+															
Sc_3CoC_4 ST Sc_3CoC_4	+															
$Y_2Co_{17}C_{0.07}$ ST $Pr_2Mn_{17}C_{0.07}$		+														
$LaCo_{1.23}C_{0.77}$ ST $MgCu_2$			+													
~$Tb_4Co_2C_5$ ST is unknown										+						
Number of phases	**3**	**4**	**2**	**1**	**1**	**1**	**1**		**3**	**4**	**3**	**3**	**2**	**2**	**2**	**2**

ST – structure type;
LTM – low temperature modification (polymorph); HTM – high temperature polymorph.

The phase equilibria of the ternary system Tb−Co−C have been studied in the limited concentration range Tb−C−TbC_2−$TbCo_5$ at 827 °C [10]. There was also a brief report on isothermal sections at 800 °C and partially at 600°C (in a region of a liquid phase at 800 °C) of the Tb−Co−C phase diagram [12]. The binary compound $TbCo_5$ was defined as unstable at 800 °C. Four ternary compounds have been detected in the annealed alloys: $TbCoC_2$ (structure type (ST) $CeNiC_2$, space group (SG) *Amm*2, *a* = 3.5749 Å, *b* = 4.5191 Å, *c* = 6.0489 Å [12]; *a* = 3.573 Å, *b* = 4.518 Å, *c* = 6.048 Å [13]; $TbCoC_{0.93}$ (ST YCoC, *a* = 3.6501 Å, *c* = 6.9276 Å [14]; *a* = 3.6523 Å, *c* = 6.931 Å for the equiatomic composition TbCoC [15]), and two other ternaries with tentative compositions ~ $Tb_5Co_2C_4$ and ~$Tb_5Co_2C_5$ as well. Later, the composition and crystal structure of ~$Tb_5Co_2C_4$ was determined as Tb_2CoC_2 with monoclinic original structure type, SG *P*2/*m*, *a* = 3.5496 Å,

b = 3.6416 Å, c = 12.3451 Å, β = 90.407° [16, 3]. However, its crystal structure was studied by X-ray powder diffraction only, which did not allow for the precise localization of the light carbon atoms. Recently, the crystal structure was reinvestigated using the neutron powder diffraction technique. Its composition was refined to $Tb_4Co_2C_3$ with a monoclinic structure: SG $P2/m$, a = 12.8149 Å, b = 3.6425 Å, c = 7.1023 Å, β = 105.601°[17].

It was reported [18, 3] that XRD pattern of compound ~$Tb_5Co_2C_4$ was indexed with the orthorhombic symmetry in a primitive Bravais lattice, a = 13.114 Å, b = 14.141 Å, c = 3.6401 Å. Using the data of EDX analysis, its tentative composition was shifted to ~$Tb_4Co_2C_5$ according to the as-weighted sample composition that exhibited the highest concentration of the phase.

This paper aims to study the phase equilibria at 800 °C of the Tb−Co−C system, taking into account all the data mentioned above.

Boundary binary systems have been studied extensively. The Tb−Co phase diagram was reported in [19]. Eight binary compounds occur in the system. Their compositions and crystal structure characteristics are presented in Table 2. For two of them, $TbCo_2$ and Tb_2Co_{17}, two different structure types were reported (Table 2). This knowledge could indicate the presence of two polymorphs for each compound. However, these data don't reflect in the indicated phase diagram.

Table 2

Crystal chemical characteristics of the Tb–Co and Tb–C binary compounds

Compound	Structure type	Pearson symbol	Space group	Unit cell parameters, Å			References
				a	*b*	*c*	
Tb_3Co	Fe_3C	*o*P16	*Pnma*	6.985	9.380	6.250	20
$Tb_{12}Co_7$	$Ho_{12}Co_7$	*mP*38	$P2_1/c$	8.39	11.32 β = 138.8°	13.97	21
Tb_4Co_3	Ho_4Co_3	*hP*22	$P6_3/m$	11.49		4.005	20
$TbCo_2$	$TbFe_2$	*hR*18	*R*-3*m*	5.093		12.514	22
	$MgCu_2$	*cF*24	*Fd*-3*m*	7.200			23
$TbCo_3$	$PuNi_3$	*hR*36	*R*-3*m*	5.011		24.38	20
Tb_2Co_7	β-Gd_2Co_7	*hR*54	*R*-3*m*	5.008		36.18	20
$TbCo_5$	$CaCu_5$	*hP*6	*P6/mmm*	4.947		3.982	24
Tb_2Co_{17}	Th_2Ni_{17}	*hP*38	$P6_3/mmc$	8.34		8.19	25
	Th_2Zn_{17}	*hR*57	*R*-3*m*	8.357		12.186	26
HT-βTbC_2	KCN	*cF*8	*Fm*-3*m*	5.691			28, 29
LT-αTbC_2	CaC_2	*tI*6	*I4/mmm*	3.690		6.217	28, 29
				3.6866		6.2034	30
Tb_2C_3	Pu_2C_3	*cI*40	*I*-43*d*	8.259			30
				8.2526			31
Tb_4C_5	αY_4C_5	*oP*18	*Pbam*	6.608	11.973	3.6871	32
				6.6172	11.985	3.6946	30
Tb_3C_4	Sc_3C_4	*tP*70	*P4/mnc*	8.1555		15.964	30
HT-βTb_2C_x (TbC_x)	NaCl	*cF*8	*Fm*-3*m*	5.107			33
				5.108			30
LT-αTb_2C_x (0.96< *x*	*anti*-$CdCl_2$	*hR*9	*R*-3*m*	3.595−3.584		18.19−18.04	34, 35
				3.6001		18.018	30

According to our studies [3], another binary compound, $TbCo_5$, is not stable at 800°C, which is also inconsistent with the Tb−Co phase diagram, where this compound is shown to occur down to room temperature. Thus, as the controversial reports indicate, further study is required to determine the temperature limits of $TbCo_5$.

Recently, the authors of [27] reinvestigated the Tb−Co phase diagram by a combination of scanning electron microscopy (SEM), electron probe microanalysis (EPMA), X-ray diffraction (XRD), and differential thermal analysis (DTA). Eight binary compounds presented in Table 2 were confirmed. Three of them Tb_3Co, $TbCo_3$ and Tb_2Co_{17} melt congruently. These data are inconsistent with those of Ref. [19] where only Tb_2Co_{17} was found to melt congruently. In [27] there were confirmed our data on $TbCo_5$ [3], however proper temperature limits of occurring $TbCo_5$ are absent.

No phase diagram is known for the Tb–C system. However, several binary terbium carbides were synthesized, and their crystal structure data were reported (Table 2). The list of references on Tb−C binary carbides, along with a detailed analysis, is presented in [3]. To our data the compounds LT-αTbC_2, Tb_2C_3, Tb_3C_4 and Tb_4C_5 are stable at 600 °C and 800 °C [12, 30]. Two polymorphs of hypocarbide LT-αTb_2C and HT-βTbC_x were detected in the alloys at 800 °C [12, 30], while only the LT-αTb_2C was found to exist at 600 °C [12].

Part of the Co−C phase diagram in the range of up to 20 at. % C is known [36]. The phase diagram is of eutectic type, with limited carbon solubility in solid cobalt. Stable binary compounds do not occur.

2. Materials and methods of the experiment

The samples were prepared by arc melting compressed pellets consisting of terbium and cobalt metals and graphite powders (with a purity of at least 99.9 wt. %) under argon purified with a molten titanium getter on a water-cooled copper hearth, using a non-consumable tungsten electrode. Weights of powders (with an accuracy of 0.001 g) of the initial elements were thoroughly mixed and transferred into a pressing mould. The powders were pressed at room temperature at a pressure of 10 MPa. Losses during pellet preparation did not exceed 0.1 wt. %. A small mass excess of carbon of up to 2 wt. % of the nominal weight of the specimen was added to avoid possible losses during the preparation of the alloys. During the melting procedure, the weight losses were less than 2 wt. % of the nominal composition of the ingot. Homogeneity was ensured by repeated melting and by flipping the ingots between the melts. Subsequently, the alloys were homogenized in evacuated quartz ampoules at 800 °C for one to two months, followed by rapid quenching in water without breaking the ampoules.

All synthesized specimens were characterized by powder X-ray diffraction (PXRD) using DRON-2.0 M (Fe *K*α- radiation). Phase analysis of the alloys and crystal structure refinements were performed with the help of WinXPOW [37] and WinCSD [38] software packages. Selected PXRD data were collected with DRON-2.0M (Fe *K*α-radiation), STOE STADI P (Cu $K\alpha_1$- and Mo $K\alpha_1$- radiation) and Huber G670 (Cu $K\alpha_1$- radiation) powder diffractometers.

SEM and qualitative and quantitative composition analyses of powders (with an accuracy of 2 at. % for metal element) were performed using energy-dispersive X-ray spectroscopy (EDX) with an elemental analyzer, REMMA-102-02, coupled to the SEM.

Differential thermal analysis (DTA) measurements were carried out under an argon atmosphere using the Linseis STA PT 1600 device. A ceramic (Al_2O_3) crucible containing 45.5(5) mg of the sample was heated up to 1360 °C and cooled down to room temperature at a constant heating and cooling rate of 10 °C/min in one cycle. The thermal effects of phase transitions, as determined from the DTA curves, were evaluated by the device software with an accuracy of ±0.1 °C.

3. Results and discussion

3.1. Binary Tb−Co and Tb−C systems

There were prepared 7 binary (in the systems Tb−Co and Tb−C) and 32 ternary alloys. All of them, after homogenizing at 800 °C, have been studied by powder XRD, and SEM has also analyzed the majority of them. Their nominal and phase compositions are presented in Fig. 1 and Table 3.

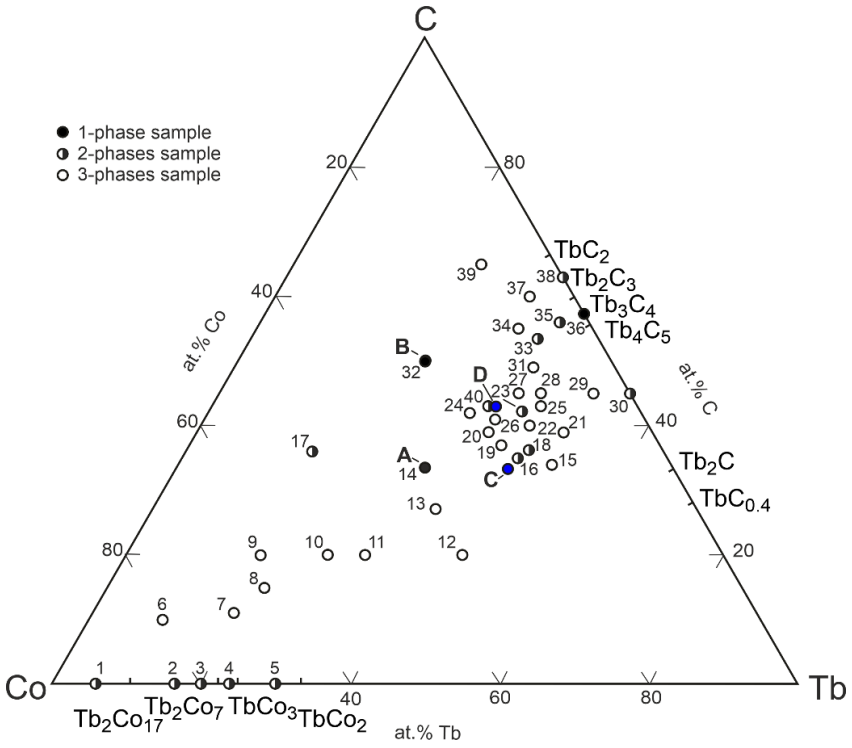

Fig. 1. Nominal and phase composition of prepared alloys. The alloy numbers in Fig. 1 correspond to the numbers in Table 3. Compositions of ternary compounds: A – TbCoC; B – $TbCoC_2$; C – $Tb_4Co_2C_3$; D – $Tb_8Co_4C_9$

Nine binary compounds Tb_2Co_{17} (ST Th_2Zn_{17}), Tb_2Co_7 (ST Gd_2Co_7), $TbCo_3$ (ST $PuNi_3$), $TbCo_2$ (ST $MgCu_2$), αTbC_2 (ST CaC_2), Tb_2C_3 (ST Pu_2C_3), Tb_3C_4 (ST Sc_3C_4), Tb_4C_5 (ST αY_2C_5), and Tb_2C (ST *anti*-$CdCl_2$) have been confirmed and detected at 800 °C.

Table 3

Nominal and phase compositions of alloys according to XRD and SEM analyses

Alloy No.	Composition		Alloy No.	Composition	
	nominal	phases		nominal	phases
1	Tb_6Co_{94}	Tb_2Co_{17}, Co	13	$Tb_{38}Co_{35}C_{27}$	$Tb_4Co_2C_3$, TbCoC, $TbCo_2$
2	$Tb_{16,6}Co_{83,4}$	Tb_2Co_{17}, Tb_2Co_7	14	$Tb_{33.4}Co_{33.3}C_{33.3}$	TbCoC
3	$Tb_{20}Co_{60}$	Tb_2Co_{17}, Tb_2Co_7	15	$Tb_{50}Co_{16}C_{34}$	$Tb_4Co_2C_3$, Tb_4C_5, Tb_2C
4	$Tb_{24}Co_{76}$	Tb_2Co_7, $TbCo_3$	16	$Tb_{45}Co_{20}C_{35}$	$Tb_4Co_2C_3$, $TbC_{0.4}$
5	$Tb_{30}Co_{70}$	$TbCo_3$, $TbCo_2$	17	$Tb_{17}Co_{37}C_{36}$	$TbCoC_2$, Co
6	$Tb_{10}Co_{80}C_{10}$	$TbCoC_2$, Tb_2Co_{17}, Co	18	$Tb_{46}Co_{18}C_{36}$	$Tb_4Co_2C_3$, Tb_4C_5 (non-equilibrium alloy)
7	$Tb_{19}Co_{70}C_{11}$	$TbCoC_2$, Tb_2Co_{17}, Tb_2Co_7	19	$Tb_{42}Co_{21}C_{37}$	TbCoC, $Tb_4Co_2C_3$, $Tb_8Co_4C_9$
8	$Tb_{21}Co_{64}C_{15}$	$TbCoC_2$, Tb_2Co_{17}, Tb_2Co_7	20	$Tb_{39}Co_{22}C_{39}$	TbCoC, $Tb_4Co_2C_3$, $Tb_8Co_4C_9$
9	$Tb_{18}Co_{62}C_{20}$	$TbCoC_2$, Tb_2Co_{17}, Tb_2Co_7	21	$Tb_{49}Co_{12}C_{39}$	$Tb_4Co_2C_3$, Tb_4C_5, Tb_2C
10	$Tb_{27}Co_{53}C_{20}$	TbCoC, $TbCo_3$, $TbCo_2$	22	$Tb_{44}Co_{16}C_{40}$	TbCoC, $Tb_4Co_2C_3$, Tb_4C_5
11	$Tb_{32}Co_{48}C_{20}$	TbCoC, $TbCo_3$, $TbCo_2$	23	$Tb_{42}Co_{16}C_{42}$	$Tb_8Co_4C_9$, Tb_4C_5 (non-equilibrium alloy)
12	$Tb_{45}Co_{35}C_{20}$	$Tb_4Co_2C_3$, $TbCo_2$, Tb_2C	24	$Tb_{35}Co_{23}C_{42}$	TbCoC, $TbCoC_2$, $Tb_8Co_4C_9$
25	$Tb_{44}Co_{13}C_{43}$	$Tb_4Co_2C_3$, $Tb_8Co_4C_9$, Tb_4C_5	33	$Tb_{38}Co_8C_{54}$	$TbCoC_2$, Tb_4C_5
26	$Tb_{39}Co_{20}C_{41}$	TbCoC, $Tb_4Co_2C_3$, $Tb_8Co_4C_9$	34	$Tb_{35}Co_{10}C_{55}$	$TbCoC_2$, Tb_2C_3, Tb_3C_4
27	$Tb_{40}Co_{15}C_{45}$	$Tb_4Co_2C_3$, $Tb_8Co_4C_9$, Tb_4C_5	35	$Tb_{40}Co_4C_{56}$	$TbCoC_2$, Tb_3C_4
28	$Tb_{43}Co_{12}C_{45}$	$Tb_4Co_2C_3$, $Tb_8Co_4C_9$, Tb_4C_5	36	$Tb_{43}C_{57}$	Tb_3C_4
29	$Tb_{50}Co_5C_{45}$	$Tb_4Co_2C_3$, Tb_4C_5, Tb_2C	37	$Tb_{34}Co_6C_{60}$	$TbCoC_2$, TbC_2, Tb_2C_3
30	$Tb_{55}C_{45}$	Tb_4C_5, Tb_2C	38	$Tb_{37}C_{63}$	TbC_2, Tb_2C_3
31	$Tb_{40}Co_{11}C_{49}$	$Tb_8Co_4C_9$, Tb_4C_5, $TbCoC_2$	39	$Tb_{25}Co_{10}C_{65}$	$TbCoC_2$, TbC_2, C
32	$Tb_{25}Co_{25}C_{50}$	$TbCoC_2$	40	$Tb_{37}Co_{20}C_{43}$	$Tb_8Co_4C_9$, TbCoC

During the study of binary Tb−Co and ternary Tb−Co−C systems at 800 °C, no $TbCo_5$ compound was found. It should be noted that at temperatures above 1200 °C, the authors of Ref. [39] identified a narrow homogeneity range of the compound, corresponding to the composition $TbCo_{5.1}$, which was attributed to the $Tb_{0.78}Cu_{5.44}$-type of structure. The cast alloy of composition $Tb_{20}Co_{80}$, which is close to the stoichiometric composition of $TbCo_5$, was found to consist of two phases: $TbCo_5$ (58 wt. %) + Tb_2Co_7 (42 wt. %) (see Fig. 2). During annealing the alloy the $TbCo_5$ phase gradually decomposed, and instead the Tb_2Co_{17} phase (ST Th_2Zn_{17}) was formed (Fig. 3).

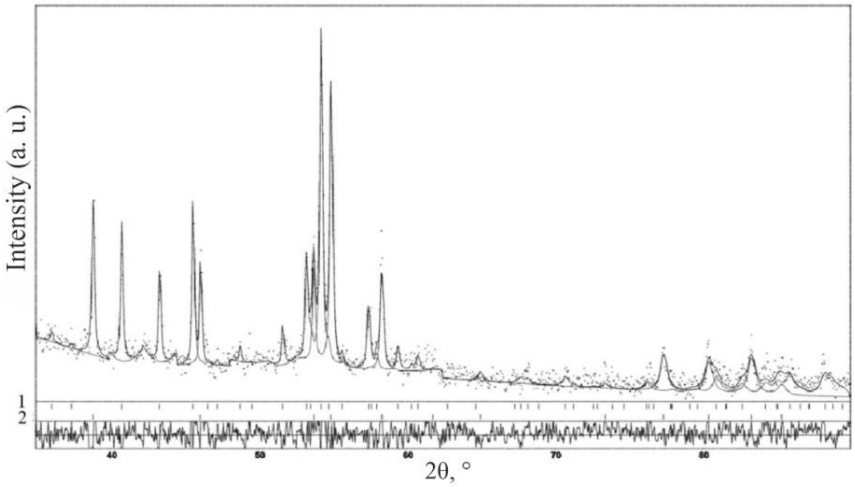

Fig. 2. Experimental (dots), theoretical (line) and difference (bottom) XRD patterns (Fe *K*α-radiation) of the as-cast alloy 3. $Tb_{20}Co_{80}$ (R_p = 19.6 %). Marked diffraction peak positions are for the phases: *1* – Tb_2Co_7 (R_I = 12.2 %); *2* – $TbCo_5$ (R_I = 7.4 %)

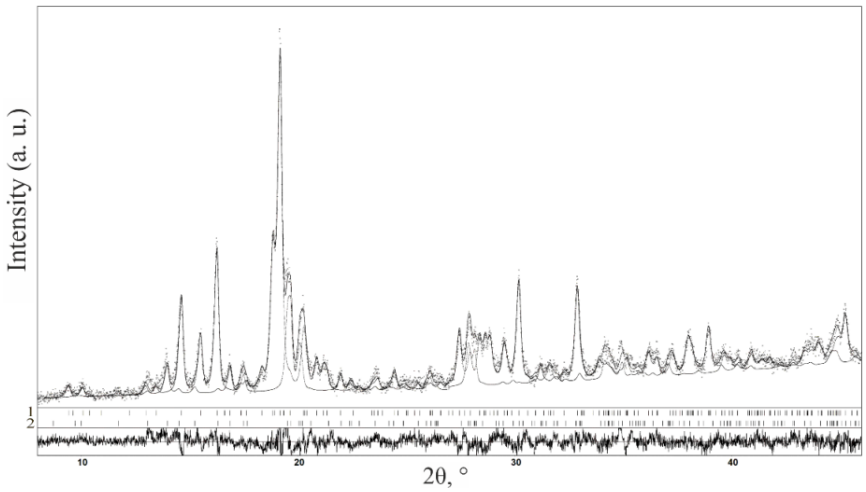

Fig. 3. Experimental (dots), theoretical (line) and difference (bottom) XRD patterns (Mo $K\alpha_1$-radiation) of the annealed at 800 °C for 1 month alloy 3. $Tb_{20}Co_{80}$ (R_p = 16.8 %). Marked diffraction peak positions are for the phases: *1* – Tb_2Co_7 (R_I = 7.1 %); *2* – Tb_2Co_{17} (R_I = 9.2 %)

To confirm the instability of $TbCo_5$ at 800°C, we performed a DTA analysis of the sample 3. $Tb_{20}Co_{80}$. Its DTA curve is shown in Fig. 4, and the interpretation of the results obtained is given in Table 4. As a result, part of the Tb−Co phase diagram was refined. It is presented in Fig. 5. The $TbCo_5$ compound melts congruently at 1335 °C, as evidenced by a significant thermal effect on the DTA curve during cooling the sample. The phase analysis of the specimen after DTA-cycle revealed nearly single-phase $TbCo_5$ composition with minor Tb_2O_3-traces resulted from the sample surface oxidizing at high temperature. However, it was impossible to record a thermal effect that could indicate decomposition of this compound by eutectoid reaction: $TbCo_5 \leftrightarrow Tb_2Co_7 + Tb_2Co_{17}$. Perhaps, this solid-state reaction occurs very slowly with a low-energy effect. After the DTA cycle, the XRD pattern of the sample 3. $Tb_{20}Co_{80}$ exhibited the presence of the main phase $TbCo_5$, along with a Tb_2O_3 impurity phase.

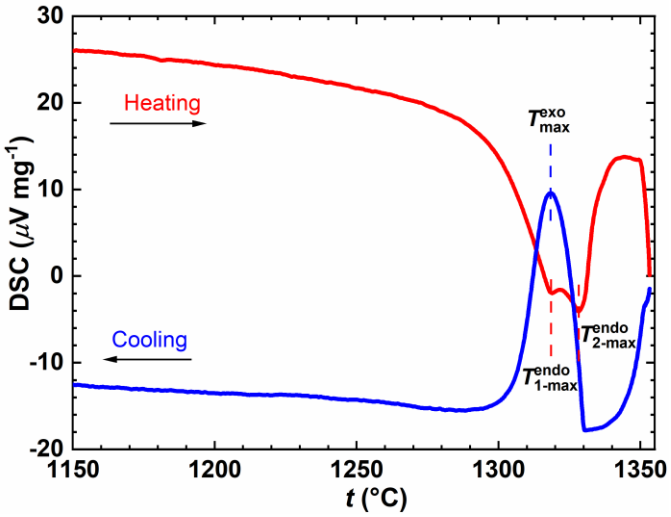

Fig 4. DTA curve (10 °C/min) for annealed at 800 °C for 1 month alloy 3. $Tb_{20}Co_{80}$

Table 4

Temperatures of phase transformations in the alloy 3. $Tb_{20}Co_{80}$ according to DTA data

Heating		Cooling	
Temperature interval	Reaction	Temperature interval	Reaction
1312.1–1322.7 °C 1324.9–1331.5 °C	$Tb_2Co_7 \rightarrow TbCo_5 + L$ $TbCo_5 \rightarrow L$	1328.9–1320.6 °C	$L \rightarrow TbCo_5$

Thus, it was found that the compound $TbCo_5$ exists within a limited temperature range above 800 °C. A proper temperature for its decomposition needs additional study.

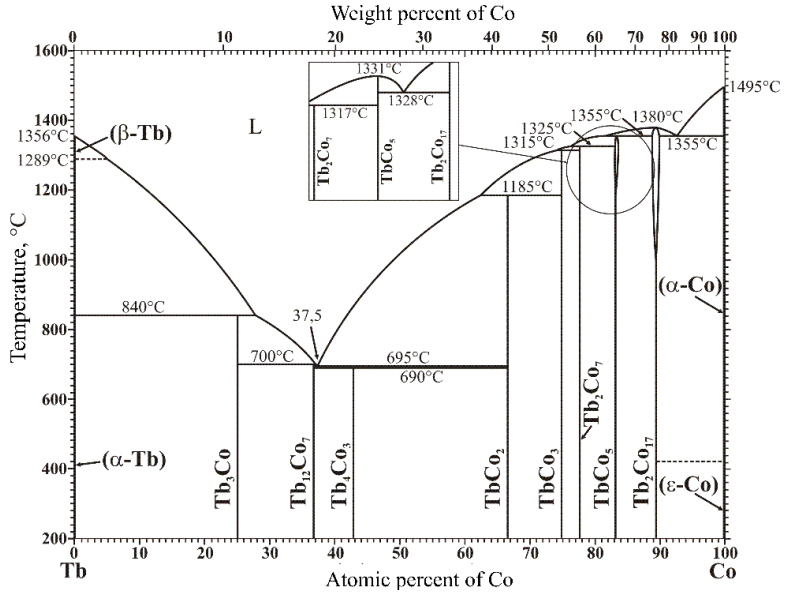

Fig. 5. Phase diagram of the Tb−Co system [19]. Inset: the refined part of it

3.2. Ternary Tb−Co−C system

Isothermal section at 800 °C of the Tb−Co−C phase diagram in the range Co−C−Tb_2C−$TbCo_2$ is shown in Fig. 6. Four ternary compounds TbCoC (A), $TbCoC_2$ (B), $Tb_8Co_4C_9$ (C), and $Tb_4Co_2C_3$ (D) have been detected. Solubility of the third component in binary Tb−Co and Tb−C compounds is absent or lesser than 1 at. %. No stable at 800 °C binary Co−C compounds were found. Compositions of ternary compounds are stable; there are no indications on their homogeneity regions at 800 °C.

The phase analysis of powder XRD patterns confirmed the literature data, reported for $TbCoC_2$ (B) and $Tb_4Co_2C_3$ (D) (Fig. 6). $TbCoC_2$ crystallizes with the orthorhombic $CeNiC_2$-type of structure, Pearson symbol (PS) *tP*8, SG *Amm*2, unit cell parameters a = 3.5749 Å, b = 4.5191 Å, c = 6.0489 Å [12, 13] and $Tb_4Co_2C_3$ belongs to the original monoclinic $Tb_4Co_2C_3$-type structure, PS *mP*18, SG *P*2/*m*, a = 12.8149 Å, b = 3.6425 Å, c = 7.1023 Å, β = 105.601° [17].

Two models were reported for the crystal structure of *R*CoC (*R* = rare earth) compounds including TbCoC: ST YCoC, SG $P4_2/mmc$, a = 3.6523 Å, c = 6.931 Å [15] and ST YCoC, SG *P*4/*mmm*, a = 3.652 Å, c = 3.465 Å [40]. However, only the lattice parameters there were reported for TbCoC in [15, 39]. The difference between these tetragonal models lies in the correct choice of the lattice parameter c, which, accordingly, leads to a change in the space group and full or half-site occupancy factor (SOF) of carbon atoms to ensure the equiatomic composition of the compound. Therefore, we performed the whole crystal structure study for it. These results are presented in ch. 3.3.

For compound D (see Fig. 6) there was reported a composition $Tb_4Co_2C_5$ and preliminary data for its crystal structure: an orthorhombic primitive Bravais lattice, a = 13.114 Å, b = 14.141 Å, c = 3.6401 Å [18, 3]. During the present study its composition was determined to be $Tb_8Co_4C_9$ as resulted from the crystal structure determination based on powder XRD data (ch. 3.4).

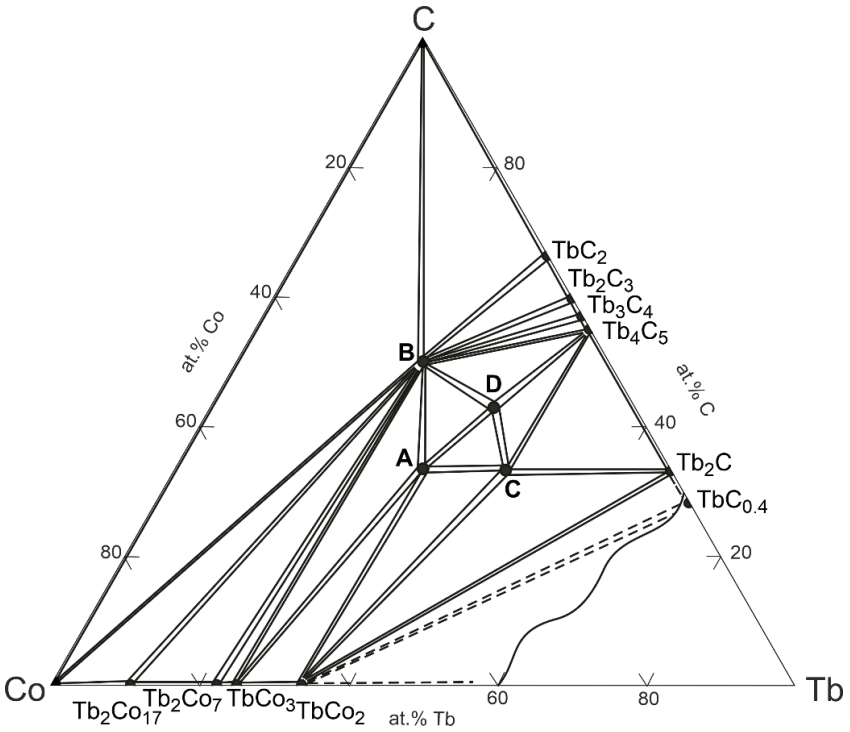

Fig. 6. Isothermal section at 800 °C of the Tb−Co−C phase diagram in the range Co−C−Tb_2C−$TbCo_2$. Ternary compounds: A – $TbCoC_{0.93}$; B – $TbCoC_2$; C – $Tb_4Co_2C_3$; D – $Tb_8Co_4C_9$

3.3. Crystal structure of TbCoC

A single-phase sample of the TbCoC compound has been synthesized (alloy 14. $Tb_{33.4}Co_{33.3}C_{33.3}$). According to Ref. [15], the condition for doubling the lattice parameter *c* was presence of the [1 0 1] superstructure *h k l* reflexion in XRD pattern. This model was confirmed for the TbCoC sample 14. The refined XRD profile for TbCoC is shown in Fig. 7. Details of this refinement are given in Table 5. An overestimated value of the isotropic displacement parameter (3.6 $Å^2$) for carbon atoms was found. Therefore, the SOF of the 2*c* site occupied by C was refined to 0.93(5) resulting in decrease in B_{iso} to 2.8(9) $Å^2$ and a composition $TbCoC_{0.93}$ for a compound A (Fig. 6). This value is consistent with the data for YCoC [15], for which a slight deviation from the equiatomic composition was found.

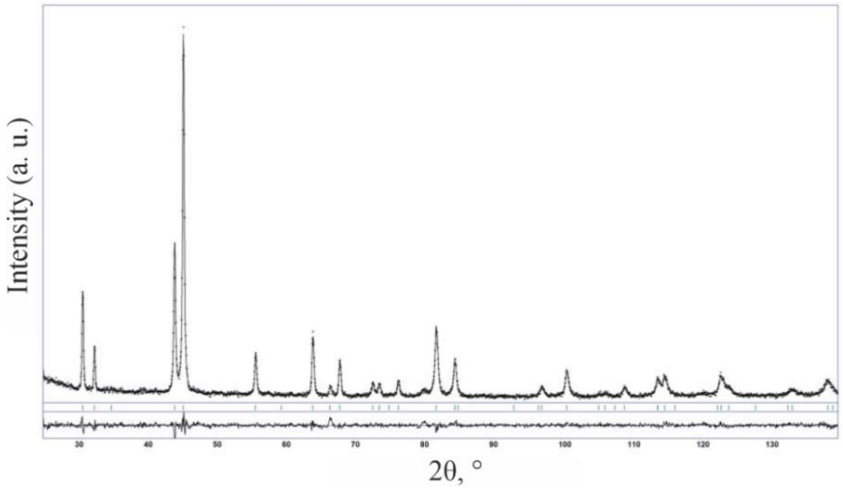

Fig. 7. Experimental (dots), theoretical (line) and difference (bottom) XRD patterns (Fe *K*α- radiation) of the annealed at 800 °C for 1 month alloy 14. $Tb_{33.4}Co_{33.3}C_{33.3}$

Table 5

Details of data collection and refinement of powder XRD pattern of the sample 14. $Tb_{33.4}Co_{33.3}C_{33.3}$

Refined composition	$TbCoC_{0.93(5)}$
Pearson symbol; and *Z*	*tP*6; 2
Space group	$P4_2/mmc$ (No. 131)
Structure type	YCoC [15]
Lattice parameters:	
a, Å	3.6501(1)
c, Å	6.9276(3)
V, Å^3	92.299(8)
Density, g/cm^3	8.2385(8)
Radiation; wavelength Å	Fe *K*α; 1.93736
Diffractometer	DRON-2.0M
$2\theta_{max}$; $sin\theta/\lambda_{max}$	140.0; 0.485
Scanning step 2θ(°); time/step (s/°)	1.0; 60
Number of refined parameters	
all; free	24; 4
Limits of *h k l*	$0\leq h\leq2$; $0\leq k\leq3$; $0\leq l\leq6$
Residuals (%): R_I; R_p; R_{wp}	4.2; 10.9; 11.0

The coordinates of atoms and their isotropic displacement parameters are listed in Table 6.

Table 6

Coordinates and isotropic parameters of atoms in the structure of $TbCoC_{0.93}$

Atom	Wyckoff site	Site occupancy factor (SOF)	*x*	*y*	*z*	B_{iso}, Å^2
Tb	2*f*	1	1/2	1/2	1/4	0.65(4)
C	2*c*	0.93(5)	0	1/2	0	2.8(9)
Co	2*a*	1	0	0	0	1.03(8)

Fig. 8 shows the unit cell and coordination polyhedra of atoms in the structure of TbCoC. Carbon atoms occupy octahedral voids formed by metal atoms and, thus, there are no contacts C−C in the structure. This explains stability of compound in air.

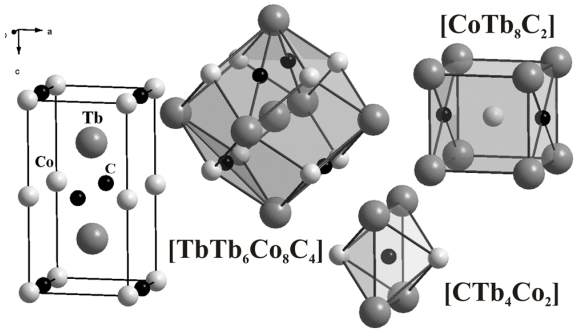

Fig. 8. Unit cell and coordination polyhedra of atoms in the structure of TbCoC

3.4. Crystal structure of $Tb_8Co_4C_9$

During the study of powder XRD and EDX analysis data for alloys in the vicinity of composition "$Tb_2Co_4C_5$" of the reported in [18] compound D (see Fig. 6) there was eliminated the sample No. 40. $Tb_{37}Co_{20}C_{43}$ (see Table 3) has the highest content of this ternary phase. The XRD pattern and microstructure of the sample are shown in Fig. 9, and the details of data collection and refinement of the pattern are listed in Table 7. The main peaks in the PXRD pattern of sample 40. $Tb_{37}Co_{20}C_{43}$ (Fig. 9) are from the primary phase D − $Tb_8Co_4C_9$. They could be indexed using a monoclinic unit cell (SG *P*2/*m*) with parameters a = 13.5621(2) Å, b = 3.64432(9) Å, c = 7.0691(1) Å, and β = 105.241(3). The sample 40 also contains the TbCoC phase as a minor one (6.6 wt. %).

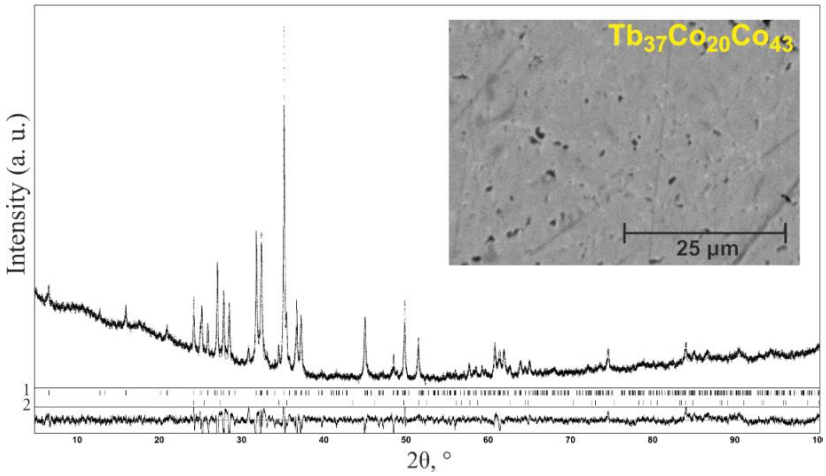

Fig. 9. Experimental (dots), theoretical (red line) and difference (bottom blue line) XRD patterns (Cu $K\alpha_1$- radiation) of the annealed at 800 °C for 1 month alloy 40. $Tb_{37}Co_{20}C_{43}$ (R_p = 2.3 %). Marked diffraction peak positions are for the phases: *1* – $Tb_8Co_4C_9$ (R_I = 11.6 %); *2* – $TbCoC_{0.93}$ (R_I = 9.4 %). Inset: microstructure of alloy: the present phases (according to EDX data) are $Tb_8Co_4C_9$ (light, main phase) and $TbCoC_{0.93}$ (grey, minority phase). Tiny black inclusions are surface defects

Table 7

Details of data collection and refinement of powder XRD pattern of the sample 40. $Tb_{37}Co_{20}C_{43}$

Refined composition	$Tb_8Co_4C_9$
Phase content, wt. %	93.8
Pearson symbol; and *Z*	*mP*21; 1
Space group	*P*2/*m* (No 10)
Structure type	$Tb_8Co_4C_9$
Lattice parameters:	
a, Å	13.5621(1)
b, Å	3.64432(9)
c, Å	7.0691(1)
β, °	105.241(3)
V, Å^3	337.10(2)
Density, g/cm^3	7.9560(5)
Radiation; wavelength Å	Cu $K\alpha_1$; 1.54056
Diffractometer	Image Plate Huber G670
$2\theta_{max}$; $sin\theta/\lambda_{max}$	100.50; 0.499
Number of refined parameters	32
Goodness-of-fit	1.01
Limits of *h k l*	$0\leq h \leq 13$; $0\leq k \leq 2$; $0\leq l \leq 7$
Residuals (%): R_I; R_p; R_{wp}	11.6; 2.3; 3.7

Having the higher carbon content in $Tb_8Co_4C_9$ compared with $Tb_4Co_2C_3$ and the same ratio of Tb:Co = 2:1 content, considering the EDX data (Fig. 9), a structure model for $Tb_8Co_4C_9$ was constructed and subsequently refined (Fig. 10, Tables 7 and 8), assuming that carbon atoms fully occupy all octahedral voids in the structure. Taking into account the limited quality of the powder XRD pattern, the atomic coordinates and displacement parameters of the carbon atoms could not be reliably refined. Fig. 10 shows the unit cell and some coordination polyhedra of atoms in the structure of $Tb_8Co_4C_9$.

Table 8

Coordinates and isotropic parameters of atoms in the structure of $Tb_8Co_4C_9$

Atom	Wyckoff site	SOF	*x*	*y*	*z*	B_{over}, Å^2
Tb1	2*n*	1.0	0.2332(4)	1/2	0.098(1)	1.03(2)
Tb2	2*n*	1.0	0.5016(8)	1/2	0.247(1)	1.03(2))
Tb3	2*n*	1.0	0.2187(4)	1/2	0.604(1)	1.03(2)
Tb4	2*m*	1.0	0.0347(3)	0	0.754(2)	1.03(2)
Co1	2*m*	1.0	0.3671(7)	0	0.430(4)	1.03(2)
Co2	2*m*	1.0	0.3615(8)	0	0.92707	1.03(2)
C1	1*b*	1.0	0	1/2	0	1.0*
C2	1*f*	1.0	0	1/2	1/2	1.0
C3	2*m*	1.0	0.158(5)	0	0.24(1)	1.0
C4	1*d*	1.0	1/2	0	0	1.0
C5	2*n*	1.0	0.3657	1/2	5/12	1.0
C6	2*m*	1.0	0.22036	0	0.8521	1.0

* Fixed B_{over} parameter for all carbon atoms.

Both the PXRD pattern and the unit cell parameters are similar to those of the related compound C − $Tb_4Co_2C_3$ [17]. The crystal structure of $Tb_8Co_4C_9$ can be described as a stacking of two fragments, formed by cobalt-centred cubic coordination polyhedra (CP) along direction *a*. Fragment *A* consists of two flat layers of Tb8 distorted cubes with two carbon atoms, which are located on opposite Tb_4/Tb_4 faces and lie nearly within the faces without creating additional adges, CPs Co@Tb_8C_2. The same CPs Co@Tb_8C_2 occur in the structure of TbCoC (if assuming SOF = 1 for C, see Fig. 8). Another fragment *B* consists of one layer, which is formed by Tb_6 octahedra, centred by carbon atoms C@Tb_6. These octahedra share triangle faces with square pyramids, the basic faces of which, Tb_4, are shared with faces of cubes from fragment *A*. In this way, layers *A* and *B* are connected. Voids in the Tb sublattice in fragment *B* are half-filled with carbon atoms, inherent to the crystal structure of TbC_x (ST NaCl). Thus, the structure of $Tb_8Co_4C_9$ can be described as a one-dimensional hybrid structure consisting of fragments *A* and *B* in a sequence ...*ABAB*… along direction *a*.

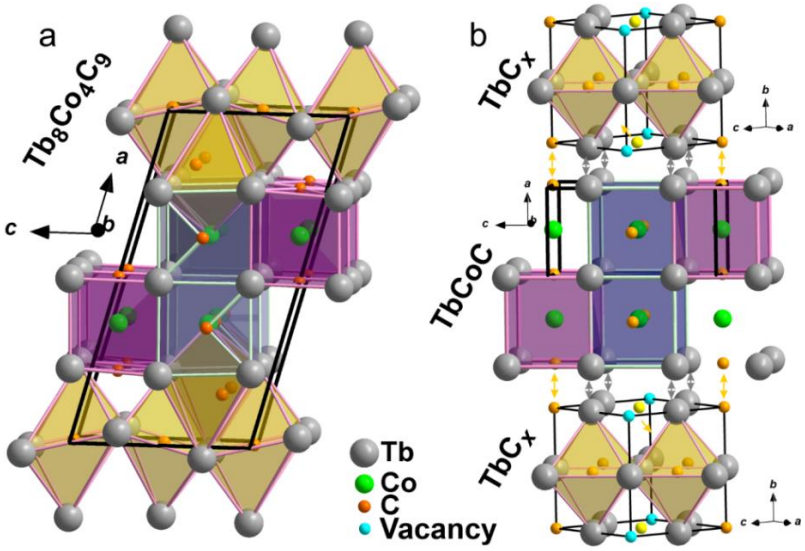

Fig. 10. Unit cell with selected coordination polyhedra of atoms in the crystal structure of $Tb_8Co_4C_9$ showing its relation to the structures of ternary TbCoC and binary TbC_x carbides *(a)*; "Intergrowth contacts" in respective TbCoC and TbC_x atomic layers are marked by arrows *(b)*. Ordered defects and C-atoms displacement in the NaCl-type TbC_x-fragment are emphasized, accordingly

All terbium atoms in the crystal structure of $Tb_8Co_4C_9$ are located at the centres of distorted cuboctahedra formed exclusively by Tb atoms. Additional Tb vertices are present in front of the faces containing Co atoms. The carbon atoms lie nearly within the square faces of these distorted cuboctahedra without forming additional edges. The cobalt atoms adopt cubic coordination, with two carbon atoms positioned on opposite Tb4 faces of the cube. The C3 and C6 atoms exhibit octahedral Tb_4Co_2 coordination, whereas distorted Tb_6 octahedra surround the remaining carbon atoms.

As one can see from Table 9, the distances are close to the sums of the respective atomic radii of the elements (r_{Tb} = 1.78 Å, r_{Co} = 1.25 Å, r_C = 0.77 Å) [41]. Tb–C distances range from 2.43(4) to 2.673 Å (most frequent values 2.43–2.57 Å) are in good agreement with the expected sum $r_{Tb} + r_C$ = 2.55 Å. Co–C distances within the distorted cubes are significantly shorter than the sum of the atomic radii: Co2–C4 = 1.81(1) Å, Co1–C5 = 1.825 Å, and Co2–C6 = 1.848 Å ($r_{Co} + r_C$ = 2.02 Å). This systematic shortening of ~0.17–0.21 Å is typical for cobalt in cubic R_8 coordination capped by two carbon atoms on opposite faces and matches values observed in related phases [3, 17]. Tb–Co distances lie between 2.986(9) and 3.194 Å (most 2.99–3.15 Å), very close to the sum of metallic radii ($r_{Tb} + r_{Co}$ = 3.03 Å), confirming normal metal–metal interactions with slight variations caused by polyhedral distortion. The observed average distances (Tb–C: 2.43–2.67 Å, Co–C: 1.81–1.85 Å, Tb–Co: 2.99–3.19 Å, Tb–Tb: 3.44–3.66 Å) fully correspond to the sums of the respective atomic radii and to distances in related rare-earth metal carbides, thereby supporting the correctness of the proposed structure model of $Tb_8Co_4C_9$.

Table 9

Interatomic distances (δ) in the crystal structure of $Tb_8Co_4C_9$

Atom		δ, Å	Atom		δ, Å	Atom		δ, Å
Tb1 –	2C2	2.43(4)	Tb3 –	2C6	2.521	Co2 –	C4	1.81(1)
	C5	2.482		C5	2.673		C6	1.848
	C6	2.494		C2	2.862(6)		2Tb1	2.986(9)
	2Co2	2.986(9)		C3	3.09(5)		2Tb2	3.08(1)
	C1	3.056(6)		2Co2	3.153(7)		2Tb2	3.132(8)
	2Co1	3.14(2)		Tb1	3.441(9)		Tb3	3.153(7)
	Tb3	3.441(9)		2Tb4	3.472(7)			
	Tb2	3.51(1)		Tb1	3.638(9)	C1 –	4Tb4	2.643(7)
	2Tb4	3.610(9)		Tb3	3.6443(1)		2Tb1	3.056(6)
	Tb3	3.638(9)		Tb2	3.66(1)			
	2Tb1	3.6443(1)				C2 –	4Tb4	2.517(7)
			Tb4 –	C6	2.429		2Tb3	2.862(6)
Tb2 –	C5	2.444		2C2	2.517(7)			
	2C4	2.524(5)		C3	2.63(7)	C3 –	2Tb1	2.43(4)
	C5	2.574		2C1	2.643(7)		Tb4	2.63(7)
	2Co2	3.08(1)		2Tb3	3.472(7)		Co1	2.80(7)
	2Co1	3.09(2)		Tb4	3.47(1)		2Tb3	3.09(5)
	Co1	3.09(1)		2Tb1	3.610(9)			
	2Co2	3.132(8)		2Tb4	3.6443(1)	C4 –	2Co2	1.81(1)
	Tb2	3.49(1)		Tb4	3.82(1)		4Tb2	2.524(5)
	Tb1	3.51(1)						
	Tb2	3.57(1)	Co1 –	2C5	1.825	C5 –	2Co1	1.825
	2Tb2	3.6443(1)		C3	2.80(7)		Tb2	2.444
	Tb3	3.66(1)		4Tb2	3.09(2)		Tb1	2.482
				2Tb1	3.14(2)		Tb2	2.574
				2Tb3	3.194(1)		Tb3	2.673
						C6 –	Co2	1.848
							Tb4	2.429
							2Tb1	2.494
							2Tb3	2.521

4. Conclusions

1. The isothermal section of the Tb−Co−C phase diagram at 800 °C in the concentration range Co−C−Tb_2C−$TbCo_2$ has been constructed for the first time using powder XRD, SEM/EDX, and DTA methods.

2. Four ternary compounds exist at 800 °C: $TbCoC_2$ (ST $CeNiC_2$, SG *Amm*2), $TbCoC_{0.93}$ (ST YCoC, SG $P4_2/mmc$), $Tb_4Co_2C_3$ (own structure type, SG *P*2/*m*), and $Tb_8Co_4C_9$ (new structure type, SG *P*2/*m*). No noticeable homogeneity ranges were detected for any of them.

3. The binary compound $TbCo_5$ is unstable at 800 °C; it forms congruently at 1331 °C and decomposes below this temperature via the eutectoid reaction $TbCo_5 \leftrightarrow Tb_2Co_7 + Tb_2Co_{17}$. The proper temperature for the indicated reaction requires additional study.

4. The crystal structure of $TbCoC_{0.93}$ was refined from powder XRD data, confirming the YCoC structure type with partially occupied carbon position (SOF = 0.93(5)).

5. A new ternary carbide $Tb_8Co_4C_9$ was synthesized, and its crystal structure was solved and refined in the monoclinic space group *P*2/*m*, a = 13.5621(2) Å, b = 3.64432(9) Å, c = 7.0691(1) Å, β = 105.241(3)°. The structure is an intergrowth of two layers of TbCoC-fragments (fragment *A*) and of NaCl-type TbC*x*-fragments (*B*), with filled octahedral voids. The structure can be described as one-dimension hybrid consisting of fragments *A* and *B* in a sequence ...*ABAB*… along direction *a*. Interatomic distances in $Tb_8Co_4C_9$ (Tb–C 2.43–2.67 Å, Co–C 1.81–1.85 Å, Tb–Co 2.99–3.19 Å, Tb–Tb 3.44 – 3.66) are in good agreement with the sums of the respective metallic atomic radii and with distances observed in related rare-earth cobalt carbides, confirming the validity of the proposed structure model.

5. Acknowledgements

V. B. and B. K. thank for financial support The Simons Foundation International, Ltd. (Grant No. SFI-PD-Ukraine-00014574).

1. *Wang J. Y., Zhou Y. C.* Recent progress in theoretical prediction, preparation, and characterization of layered ternary transition-metal carbides // Annu. Rev. Mater. Res. 2009. Vol. 39. P. 415−443. DOI: https://doi.org/10.1146/annurev-matsci-082908-145340
2. *Adachi G.-Y., Imanaka N., Fuzhong Z.* Chapter 99: Rare earth carbides, In: Handbook on the Physics and Chemistry of Rare Earths Including Actinides, K. A. Gschneidner Jr., L. Eyring (Eds.), Vol. 15, Elsevier Science Publishers B. V., Amsterdam, 1991. P. 61–189. DOI: https://doi.org/10.1016/S0168-1273(05)80005-4
3. *Babizhetskyy V., Kotur B., Levytskyy V., Michor H.* Chapter 298: Alloy systems and compounds containing rare earth metals and carbon. In Handbook on the Physics and Chemistry of Rare Earths Including Actinides, J.-C. G. Bünzli, V. K. Pecharsky (Eds.). North-Holland, Amsterdam, 2017. Vol. 52. P. 1–263. DOI: https://doi.org/10.1016/bs.hpcre.2017.09.001
4. *Su D. S., Centi G.* A perspective on carbon materials for future energy application // J. Energy Chem. 2013. Vol. 22. P. 151–173. DOI: https://10.1016/S2095-4956(13)60022-4

5. *Pecharskaya A. O.* Crystal Chemistry of Ternary Carbides of the Rare Earths. Abstract of Candidate's Thesis (Chemical Sciences). Lviv, 1989. 17 p. (in russian).
6. *Marusin E. P.* Investigation of ternary systems {yttrium, lanthanum, cerium}–{iron, cobalt, compounds). Abstract of Candidate's Thesis (Chemical Sciences). Lviv, 1982. 21 p. (in russian).
7. *Levytskyy V., Kostetska A., Babizhetskyy V., Kotur B. Ya., Serkiz R.* System Dy−Co−C at 800 °C // Visnyk Lviv Univ. Ser. Chem. 2013. Iss 54. Pt. 1. P. 19−27 (in Ukrainian).
8. *Tsokol' A. O.* Ternary systems Gd–{Co, Ni}–C // Visnyk Lviv Univ. Ser. Chem. 1986. Iss. 27. P. 41–43 (in Ukrainian).
9. *Levytskyi V., Babizhetskyy V., Kotur B.* System Er−Co−C at 800 °C. Crystal structures of ErC and ErCoC // Visnyk Lviv Univ. Ser. Chem. 2023. Iss. 64. P. 73–90 (in Ukrainian). DOI: https://doi.org/10.30970/vch.6401.073
10. *Putyatin A. A., Kozlovskii V. F.* Phase relations in the systems RE–Co–C at various pressures // Vestnik Mosk. Univ. Ser. 2. Khim. 1991. Iss. 32. P. 58–61 (in russian).
11. *Stadelmaier H. H., Liu N.-C.* The ternary system cobalt-samarium-carbon // Z. Metalkde. 1985. Vol. 76. P. 585–588. DOI: https://doi.org/10.1515/ijmr-1985-760901
12. *Levytskyy V. O.* The compounds of the *R*–*M*–C systems (*R* = rare earth metal, *M* = 3*d*-element) and their hydrides: synthesis, structure, and properties. Abstract of Candidate's Thesis (Chemical Sciences). Lviv, 2015. 24 p. (in Ukrainian).
13. *Jeitschko W., Gerss M. H.* Ternary carbides of the rare earth and iron group metals with $CeCoC_2$- and $CeNiC_2$-type structure // J. Less-Common Met. 1986. Vol. 116. P. 147–157. DOI: https://10.1016/0022-5088(86)90225-0
14. *Shäfer W., Wil G., Kotsanidis P. A., Yakinthos J. K.* Magnetic properties of $RCoC_2$ (*R* = Y, Gd, Tb) compounds // J. Magn. Magn. Mater. 1990. Vol. 88. P. 13–17. DOI: https://doi.org/10.1016/S0304-8853(97)90005-6
15. *Gerss M. H., Jeitschko W.* YCoC and isotypic carbides with a new, very simple structure type // Z. Naturforsch. B 41. 1986. P. 946–950. DOI: https://doi.org/10.1515/znb-1986-0804
16. *Levytskyy V., Babizhetskyy V., Kotur B.* The new structure type Tb_2CoC_2 and isotypic compounds // Coll. Abstracts of XIII International Conference on Crystal Chemistry of Intermetallic Compounds, 25–29 September. Lviv, Ukraine, 2016. P. 76.
17. *Levytskyi V., Isnard O., Kremer R. K., Babizhetskyy V., Fontaine B., Rocquefelte X., Halet J.-F., Gumeniuk R.* Crystal, electronic and magnetic structures iof a novel series of intergrowth carbometalates $R_4Co_2C_3$ (R = Y, Gd, Tb) // Dalton Trans. 2021. Vol. 50. P. 4202−4209. DOI: https://doi.org/10.1039/D1DT00420D
18. *Maliyenko R. K., Levytskyy V. O.* New compound $Tb_4Co_2C_5$ in system Tb–Co–C // Abstracts of X Ukrainian Scientific Conference for Students and Young Scientists with International Participation "Current Chemical Problems", 27–29 March. Vinnytsia, Ukraine, 2017. P. 93 (in Ukrainian).
19. Binary Alloy Phase Diagrams / Ed. by T. B. Massalski, H. Okamoto, P. R. Subramanian *et al.* ASM International, 1990. Vol. 2. 2224 p.
20. *Buschow K. H. J.* Rare-earth cobalt intermetallic compounds // Philips Res. Rep. 1971. Vol. 26. P. 49–64.
21. *Adams W., Moreau J. M., Parthe E., Schweiser J.* $R_{12}Co_7$ Compounds with R = Gd, Tb, Dy, Ho, Er // Acta Crystallogr. Sec. B. 1976. Vol. 32. P. 2697–2699. DOI: https://doi.org/10.1107/S0567740876008595

22. *Yoshimoto N., Sakurai J., Komura Y. J.* X-ray diffraction study on crystal deformation of $TbCo_2$ // J. Magn. Magn. Mat. 1983. Vol. 31/34. P. 137−139. DOI: https://doi.org/10.1016/0304-8853(83)90188-9
23. *Lee E. W., Pourarian F.* Magnetoelastic Properties of (Rare-Earth)Co_2 Compounds. I. Exchange-Striction // Phys. Stat. Solidi A: App. Res. 1976. Vol. 33. P. 483–489. DOI: https://doi.org/10.1002/pssa.2210330206
24. *Haszko S. E.* Intermediate phases with the Cu_5Ca structure // Trans. AIME. 1960. Vol. 218. P. 763.
25. *Liu J. P., Brabers V. J., Winkelman A. J. M., Menovsky A. A., De Boer F. R., Buschow K. H. J.* Synthesis and magnetic properties of $R_2Co_{17}N_x$ type interstitial compounds // J. Alloys Compd. 1993. Vol. 200. P. 3–6. DOI: https://doi.org/10.1016/0925-8388(93)90461-U
26. *Bouchet G., Laforest J., Lemaire R., Schweiser J.* Structures cristallines des composes intermetalliques Tb_2Co_{17} dans lesquels T est un metal des terres rares ou l'yttrium // Comp. Rend. Acad. Sci. Ser. B: Sciences Physiques. 1966. Vol. 262. P. 1227–1230.
27. *Bajenova I., Shakirova J., Khvan* K., *Cheverikin* V., *Zanaeva E.* Experimental investigation of the phase equilibria in the Tb−Co and Tb−Co−Fe systems and magnetic properties of phases // Mater. Today Comm. 2022. Vol. 32. Art. 103960. DOI: https://doi.org/10.1016/j.mtcomm.2022.103960
28. *Krikorian N. H., Wallace T. C., Bowman M. G.* Phase relationships of the high-carbon portion of lanthanide–carbon systems. In: Proprietes Thermodynamiques Physiques et Structurales des Derives Semi-Metalliques. CNRS, Paris, 1967. P. 489–498.
29. *Gschneidner K. A. Jr., Calderwood F. W.* The C–Tb (carbon–terbium) system // Bull. Alloy Phase Diagr. 1986. Vol. 7. P. 562–563.
30. *Levytskyy V., Hembara M., Babizhetskyy V., Kotur B.* System Tb–Cr–C at 800 °C: the phase equilibria and crystal structures of ternary compounds // Visnyk Lviv Univ. Ser. Chem. 2016. Iss. 57. Pt. 1. P. 23–33 (in Ukrainian).
31. *Atoji M., Williams D. E.* Neutron diffraction studies of La_2C_3, Ce_2C_3, Pr_2C_3, and Tb_2C_3 // J. Chem. Phys. 1961. Vol. 35. P. 1960−1966. DOI: https://doi.org/10.1063/1.1732193
32. *Czekalla R., Hüfken T., Jeitschko W., Hoffmann R.-D., Pöttgen R.* The rare earth carbides R_4C_5 with R=Y, Gd, Tb, Dy, and Ho // J. Solid State Chem. 1997. Vol. 132. P. 294–299.
33. *Spedding F. H., Gschneidner K. A. Jr., Daane A. H.* The crystal structures of some of the rare earth carbides // J. Am. Chem. Soc. 1958. Vol. 80. P. 4499–4503.
34. *Atoji M.* Magnetic and crystal structures of the trigonal Tb_2C // J. Chem. Phys. 1969. Vol. 51. P. 3872–3876. DOI: https://doi.org/10.1063/1.1672604
35. *Atoji M.* Neutron-diffraction studies of Tb_2C and Dy_2C in the temperature range 4–296 K // J. Chem. Phys. 1981. Vol. 75. P. 1434–1441. DOI: https://doi.org/10.1063/1.442150
36. *Ishida K., Nishizawa T.* The C–Co (Carbon−Cobalt) system // J. Phase Equil. 1991. Vol. 12. P. 417–424. DOI: https://doi.org/10.1007/BF02645959
37. STOE WinXPow (ver. 2.10), Stoe & Cie GmbH. Darmstadt, Germany, 2004.
38. *Akselrud L., Grin Y.* WinCSD: software package for crystallographic calculations (Version 4) // J. Appl. Crystallogr. 2014. Vol. 47. P. 803–805. DOI: https://doi.org/10.1107/S1600576714001058

39. *Velge W. A. J. J., Buschow K. H. J.* Magnetic and crystallographic properties of some rare earth cobalt compounds with $CaZn_5$ structure // J. Appl. Phys. 1968. Vol. 39. P. 1717−1720. DOI: http://dx.doi.org/10.1063/1.1656420
40. *Tsokol' A. O., Bodak O. I., Marusin E. P.* Crystal structure of YCoC // Kristallographiya. 1989. Vol. 34. P. 1014–1016 (in russian). TR: Sov. Phys. Crystallogr. 1989. Vol. 34. P. 612–614.
41. *Holleman A. F., Wiberg E., Wiberg N.* Lehrbuch der anorganischen Chemie, Walter de Gruyter. Berlin–New York, 1995. P. 1838–1840.

СИСТЕМА Tb−Co−C ПРИ 800 °C: ФАЗОВІ РІВНОВАГИ ТА КРИСТАЛІЧНА СТРУКТУРА СПОЛУК

В. Левицький[1], В. Бабіжецький[2], Б. Котур[2]

[1]Інститут експериментальної фізики, ТУ Гірнича академія Фрайберг, вул. Лейпцизька, 23, 09599 Фрайберг, Німеччина;

[2]Львівський національний університет імені Івана Франка, вул. Кирила і Мефодія, 6, 79005 Львів, Україна

За допомогою Х-променевого фазового і структурного аналізу порошку, енергодисперсійної Х-променевої спектроскопії та диференціального термічного аналізу (для сполуки $TbCo_5$) побудовано ізотермічний переріз діаграми стану системи Tb−Co−C при 800 °C в області Co−C−Tb_2C−$TbCo_2$. Виготовлено та вивчено сім подвійних та тридцять три потрійні зразки. Їх синтезовано за допомогою електродугової плавки наважок вихідних компонентів високої чистоти (> 99,9 мас. % основного компонента) в атмосфері аргону. Виготовлені сплави гомогенізовано в запаяних під вакуумом кварцових ампулах при 800 °C упродовж 1−2 місяців. Після відпалу ампули зі зразками гартували в холодній воді. За зазначеної температури у системі існують чотири тернарні сполуки постійного складу $TbCoC_2$, $TbCoC_{0,93}$, $Tb_4Co_2C_3$, $Tb_8Co_4C_9$ та дев'ять бінарних сполук Tb_2Co_{17}, Tb_2Co_7, $TbCo_3$, $TbCo_2$, TbC_2, Tb_2C_3, Tb_3C_4, Tb_4C_5, Tb_2C. Сполука $TbCo_5$ існує в обмеженому температурному інтервалі за температур, вищих за 800 °C: утворюється з розплаву при 1331 °C і розпадається за евтектоїдною реакцією $TbCo_5 \leftrightarrow Tb_2Co_7 + Tb_2Co_{17}$. Температура розпаду потребує додаткового вивчення. Кристалічна структура тернарних сполук: $TbCoC_2$ – підтверджено структурний тип (СТ) $CeNiC_2$, символ Пірсона (СП) *oS*8, просторова група (ПГ) *Amm2*, a = 3.5749 Å, b = 4.5191 Å, c = 6.0489 Å; $TbCoC_{0,93}$ вивчено методом порошку – СТ YCoC, СП *tP*6, ПГ $P4_2/mmc$, a = 3,6526(4) Å, c = 6,941(1) Å; $Tb_8Co_4C_9$ структуру вивчено методом порошку − новий (власний) структурний тип, СП *mP*21, ПГ $P2/m$, a = 13,562(2) Å, b = 3,64432 Å, c = 7,0691(1) Å, β = 105,241(3)°; $Tb_4Co_2C_3$ – підтверджено СТ $Tb_4Co_2C_3$, СП *mP*18, ПГ $P2/m$, a = 12,8149 Å, b = 3,6425 Å, c = 7,1023 Å, β = 105,601°. Проведено кристалохімічний аналіз структур сполук TbCoC та $Tb_8Co_4C_9$.

Стаття надійшла до редколегії 15.11.2025
Після доопрацювання 10.01.2026
Прийнята до друку 12.02.2026
Оприлюднена онлайн 29.05.2026